**Supporting Information**

# Curvature sensing by the epsin N-terminal homology (ENTH) domain measured on cylindrical lipid membrane tethers

Benjamin R. Capraro*, Youngdae Yoon[#], Wonhwa Cho[#], and Tobias Baumgart*
[*]Department of Chemistry, University of Pennsylvania, Philadelphia, 19104, and Department of [#]Chemistry, University of Illinois at Chicago, Chicago, Illinois 60607

*Materials and Methods*

**Protein purification** | ENTH (residues 1-158 of epsin 1) amplified by PCR was inserted into the pEGFP-N1 vector using restriction enzymes EcoRI/BamHI to achieve C-terminal GFP tagging. The fusion was then inserted into pET28-(a) with EcoRI/NotI restriction enzymes. BL21 RIL Codon Plus (Stratagene, La Jolla, CA) cells harboring this construct were grown at 37 °C in LB media. 1 mM of IPTG was added when the OD600 was 0.5-0.8. The cells were grown for additional 6 to 10 hours at 25 °C, and then harvested by centrifugation. Pellets were resuspended with 50 mM Tris-HCl (pH 7.4) containing 160 mM KCl, 1 mM phenylmethylsulfonyl fluoride, and 5 mM dithiothreitol. The cells were lysed by sonication, and fractionated by centrifugation at 38,000 *g* for 30 min at 4 °C. The supernatant was applied to a Ni-NTA resin (Qiagen), and fractions collected from an imidazole concentration gradient were further purified by ion-exchange chromatography. Purity and concentration of the recombinant protein were determined by SDS-PAGE and bicinchoninic acid assay, respectively.

**Vesicle preparation** | 1-palmitoyl-2-oleoyl-*sn*-glycero-3-phosphocholine (POPC), 1,2-distearoyl-*sn*-glycero-3-phosphoethanolamine-*N*-[biotinyl(polyethylene glycol)-2000] (ammonium salt) (Bio-PEG-DSPE), L-α-phosphatidylinositol 4,5-bisphosphate ($PIP_2$) (Brain, ammonium salt) were from Avanti (Alabaster, AL), Texas Red-1,2-dihexadecanoyl-*sn*-glycero-3-phosphoethanolamine triethylammonium salt (TR-DHPE) from Invitrogen (Carlsbad, CA), and the fluorescent $PIP_2$ variant BODIPY TMR-PtdIns(4,5)$P_2$-$C_{16}$ from Echelon Biosciences Inc. (Salt Lake City, UT). Lipids were mixed to 0.7-1 mM in 3:1 chloroform:methanol. $PIP_2$ was used at 1 mol%, TR-DHPE at 0.3 mol%, and Bio-PEG-DSPE 0.1 mol%, in liposomes with the majority lipid being POPC. Vesicles were prepared by electroformation as previously described[1, 2]. Swelling conditions were 56-60 °C with 0.26-0.4 mM lipid concentration in 240 or 300 mM sucrose solution. For measurements with fluorescent $PIP_2$ (Figure S2), asymmetric labeling of

electroswelled POPC vesicles in 100 mM sucrose at ~0.4 mol% was carried out by adding 80 μM BODIPY TMR-PtdIns(4,5)$P_2$-$C_{16}$ in methanol to 1% (v/v).

**Experimental procedure** | Micropipettes were fabricated as described[1, 2] with inner diameters 3-7 μm, filled with filtered 0.5 mg/ml fatty acid-free BSA (Sigma, St. Louis, MO) in PBS (Fisher Scientific, Newark, DE) using a Microfil needle (WPI, Sarasota, FL), rinsed with deionized water, and finally filled with filtered swelling solution. To counter vesicle-glass adhesion, coverslips were passivated using 1.5 μl of 0.5 mg/ml BSA in PBS and air dried. Vesicles were diluted 100-fold into the sucrose containing swelling solution plus ~15 mOsm total electrolyte, pH 7.4-7.6, with ENTH added to 0.2-0.5 μM, in a previously described chamber[2]. ENTH-GFP concentration on vesicles both containing and lacking Bio-PEG-DSPE was found to be indistinguishable by fluorescence microscopy, whereas no association was observed with purified GFP, or if $PIP_2$ was omitted (not shown). Vesicle aspiration and tether formation were as described[1, 2], and tethers were extended to length 6 ± 1.5 μm (depending on vesicle size and excess area) for fluorescence intensity measurements. Experiments were carried out at room temperature (22 ± 2 °C). Tension values were calculated from

$$\sigma = \Delta P \frac{R_p}{2\left(1 - R_p / R_v\right)} \qquad \text{(S1)}$$

(with $\Delta P$ the aspiration pressure, $R_p$ pipet radius, and $R_v$ vesicle radius).

For Figure S2, we determined the tether radius using a previously described tube elongation method in which changes in the projection length of the aspirated vesicle upon tube extension are measured[2], and acquired separate images for intensity analysis at corresponding tension levels. Measurements were carried out within 2 hrs of asymmetric labeling.

**Image acquisition and analysis** | To measure curvature-partitioning of ENTH-GFP, Kalman line-averaged *xz* scans near the tether base were used as demonstrated in Figure 2A[2]. Laser illumination powers (wavelengths 488 nm and 543 nm) were within regions where a linear dependence of detected emission on illumination power is found (see Figure S1). Acquisition filters were 510(10) nm and 595(20) nm.

To *xz* image data we fitted a two-dimensional Gaussian using MATLAB (Mathworks, Natick, MA), which determined the peak and background intensities, their difference yielding the values $I_{green}$ and $I_{red}$ (Figure 2, S1).

To red channel data in Figure 2, a correction for bleedthrough, namely, a subtraction of 15.3% fluorescence intensity in the green channel, has been applied. We determined this correction from measurements of ENTH-GFP-bound tethers from membranes containing no fluorescent lipid (not shown).

For Figure S2, intensity values were extracted with background subtraction from MATLAB Gaussian fitting of averaged image reconstructions comprising 8 Kalman-averaged confocal z-sections of the total tether length.

**Derivation of sorting expressions** | We adapt existing thermodynamic theory[2-6] and consider a membrane containing trace lipids that present protein binding sites. Constituting the membrane are two regions: a tether with curvature $C = 1/R$ is connected to a vesicle, i.e., a quasi-flat membrane element of large area compared to the tether. We obtain an expression for the difference in composition of the protein-binding lipid between the vesicle and the tether, which vanishes in the limit of no curvature.

The membrane free energy accounting for curvature and partitioning is:

$$F = 2\pi RL\left(\frac{\kappa_0}{2R^2} + \frac{\Lambda\Delta\phi}{R} + \sigma + \frac{1}{2}\chi^{-1}\Delta\phi^2\right) \qquad \text{(S2)}$$

Here, $\Delta\phi$ represents the increase in mole fraction on the tether of the protein-binding lipid relative to its initial value $\phi_v$. The quantity $\rho$ is the two-dimensional lipid density, assumed here to be equal for all lipids, and $L$ and $R$ are the length and radius of the tether, respectively. Furthermore, the following inverse susceptibilities have been used: $\kappa_0 = \frac{1}{A}\left(\frac{\partial^2 F}{\partial C^2}\right)_0$, $\Lambda = \frac{1}{A}\left(\frac{\partial^2 F}{\partial\phi\partial C}\right)_0$, and $\chi^{-1} = \frac{1}{A}\left(\frac{\partial^2 F}{\partial\phi^2}\right)_0$ where $A$ is the membrane area and the index indicates evaluation of the respective derivatives at zero curvature. $\Lambda$ is a curvature coupling constant[6], $\kappa_0$ is the bare membrane bending stiffness[6] and $\chi$ is the osmotic compressibility which here is

$\phi_v / \rho kT$ considering the dilute limit and entropic contributions only. Generalizations accounting for excluded volume and protein lateral interactions are readily implemented. Minimization of eq S2 with respect to $\Delta\phi$ yields:

$$\Delta\phi = -\frac{\Lambda\chi}{R} \tag{S3}$$

Furthermore, minimizing eq S2 with respect to *R* yields

$$\frac{\kappa_0}{2R^2} = \frac{\Lambda^2\chi}{2R^2} + \sigma \approx \frac{\Lambda^2\chi}{2R_0^2} + \sigma = \frac{\Lambda^2\chi\sigma}{\kappa_0} + \sigma, \tag{S4}$$

which results in

$$\frac{1}{R^2} = \frac{2\sigma}{\kappa_0}\left(1 + \frac{\Lambda^2\chi}{\kappa_0}\right) \approx \frac{2\sigma}{\kappa_0 - \Lambda^2\chi} \equiv \frac{2\sigma}{\kappa_{eff}}. \tag{S5}$$

We therefore have

$$R^{-1} = \sqrt{\frac{2\sigma}{\kappa_{eff}}}, \tag{S6}$$

where $\kappa_{eff} = \kappa_0 - \Lambda^2\chi$ embodies the effectively lowered bending stiffness arising from the curvature preference of bound proteins, as quantified by $\Lambda$. Substitution of eq S6 into eq S3 yields an expression for the composition change:

$$\Delta\phi = -\Lambda\chi\sqrt{\frac{2\sigma}{\kappa_{eff}}} \tag{S7}$$

The change in the ratio of fluorescence emission from proteins to that from lipids, $I_r = I_{green}/I_{red}$ (see main text and Figure 2B), induced by experimental modulation of curvature is related to the composition difference among tether and vesicle $\Delta\phi = \phi_t - \phi_v$ :

$$\frac{I_r^t}{I_r^v} = \frac{\phi_t}{\phi_v} = 1 + \frac{\Delta\phi}{\phi_v}, \qquad \text{(S8)}$$

where it has been assumed that fluorescence intensity is proportional to the mole fraction of the ENTH/$PIP_2$ complex. We determined the fluorescence intensity ratio $I_r^v$ of the (essentially zero curvature) vesicle from extrapolation of $I_r^t$ measurements (see Figure 2B) to zero curvature; $I_r^0 = I_r^v$. This procedure avoids having to consider different fluorophore orientations with respect to excitation and emission pathways on vesicle and tube. If $I_r^0$ were to be determined by the measurement of fluorescence intensities on the vesicle membrane, then a polarization factor would have to be experimentally determined to be able to obtain the ratio $I_r^t/I_r^0$ [4].

Fluorescence intensity measurements are binned over equal $\sqrt{\sigma}$ intervals, and linear regression is used to extract $\Lambda$ from eq 1 (contained in the main text), which is obtained from insertion of eq S7 into eq S8:

$$I_r/I_r^0 = 1 + \frac{\Delta\phi}{\phi_v} = 1 - \frac{\Lambda}{\rho kT}\sqrt{\frac{2\sigma}{\kappa_{eff}}} \qquad \kappa_{eff} = \kappa_0 - \Lambda^2\chi, \qquad \text{(1a, b)}$$

using $\kappa_0$ = 0.9x$10^{-19}$ J (ref. S2 for POPC and data from our lab not shown for membranes containing $PIP_2$) and $\rho$ = 1.47 $nm^{-2}$ (ref. S7).

We note that the Leibler curvature-composition coupling parameter $\Lambda$ can be related to spontaneous curvature. In an earlier contribution[2] we had shown that to first order the spontaneous curvature model leads to:

$$\frac{\phi_t}{\phi_v} = 1 + \frac{a_\alpha \kappa_0 C_\alpha}{kTR}, \qquad \text{(S9)}$$

where $a_\alpha = 1/\rho$ is the cross section area of molecule $\alpha$ with molecular spontaneous curvature[3] $C_\alpha$, ideally diluted in a membrane with majority lipid of negligible spontaneous curvature. From eq S3 and eq S8 we have

$$\frac{\phi_t}{\phi_v} = 1 - \frac{a_\alpha \Lambda}{kTR}, \qquad \text{(S10)}$$

and therefore one finds that $\Lambda = -\kappa_0 C_\alpha$. From the measured value of $\Lambda$ = -146 pN we have the spontaneous curvature of the ENTH/$PIP_2$ complex: $C_{ENTH/PIP2}$ = 1.6 $nm^{-1}$.

*Supporting Figures*

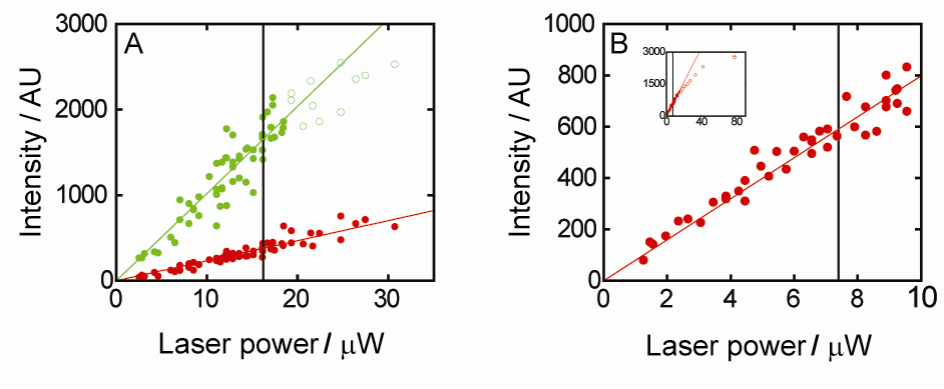


***Figure S1.*** Determination of the linear regime for detected fluorescence emission as a function of excitation power. The specimen and acquisition are as in Figures 1-2, except that blue (A) or green (B) laser illumination was exclusively used. (A) Fluorescence detected as the illumination power (at the microscope objective back aperture) from a 488 nm laser is varied. Green points report green channel fluorescence; open points distinguish data for power levels beyond the maximum for which detected emission is linearly proportional to excitation power, judged by visual inspection of the presented data and linear fitting (green line, excluding open points). Red points report detected red channel intensity, arising from (cross)-excitation of TR-DHPE by 488 nm illumination and bleedthrough of ENTH-GFP emission. The vertical line reports the maximum (wavelength λ = 488 nm) illumination power used for measurements of Figure 2,

which is within the linear regime of the data. (B) Analogous measurement to that of (A) using $\lambda$ = 543 nm illumination only. Red points report red channel fluorescence (green channel fluorescence was not detectable). The black line indicates the maximum ($\lambda$ = 543 nm) illumination power used for measurements of Figure 2. The inset includes data for the range of achievable laser powers. As in (A), open points were excluded from the linear fit (red line).

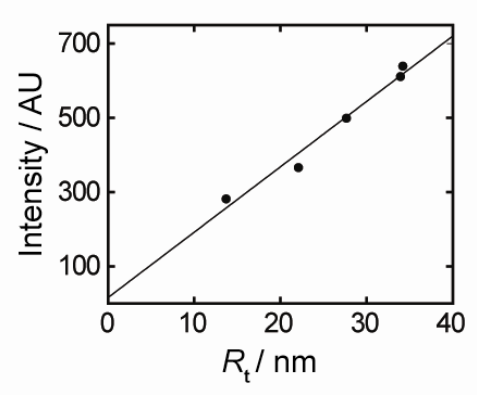


***Figure S2.*** Assessment of $PIP_2$ curvature partitioning. We applied the method of ref. S2 to BODIPY TMR-PtdIns(4,5)$P_2$-$C_{16}$ incorporated into the outer leaflet of POPC vesicles. Intensities extracted from *xyz* reconstructions of a tether as a function of its radius, in a representative individual tether. The tether radius is determined by the elongation method (refs. S2 and S8), for varied tensions. Curvature re-distribution of $PIP_2$ would produce a nonzero intercept or a nonlinear relationship between the variables plotted[2].

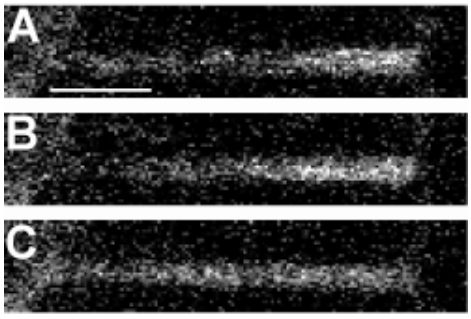


***Figure S3.*** Demonstration that migration of protein from the vesicle reservoir to the tether underlies the enrichment of ENTH on the tether studied in Figures 1-2. (A) Green channel fluorescence image of an ENTH-GFP-bound tether 5 seconds after a sudden change in tension

from $\sigma$ = 0.057 to 0.549 mN/m. The vesicle appears on the right of the images, and the polystyrene bead used in tether formation on the left. (B) 15 sec (B) 30 sec, after which no significant further fluorescence changes were observable, establishing that equilibration occurs, as in Figure 1. Bar: 2 μm.

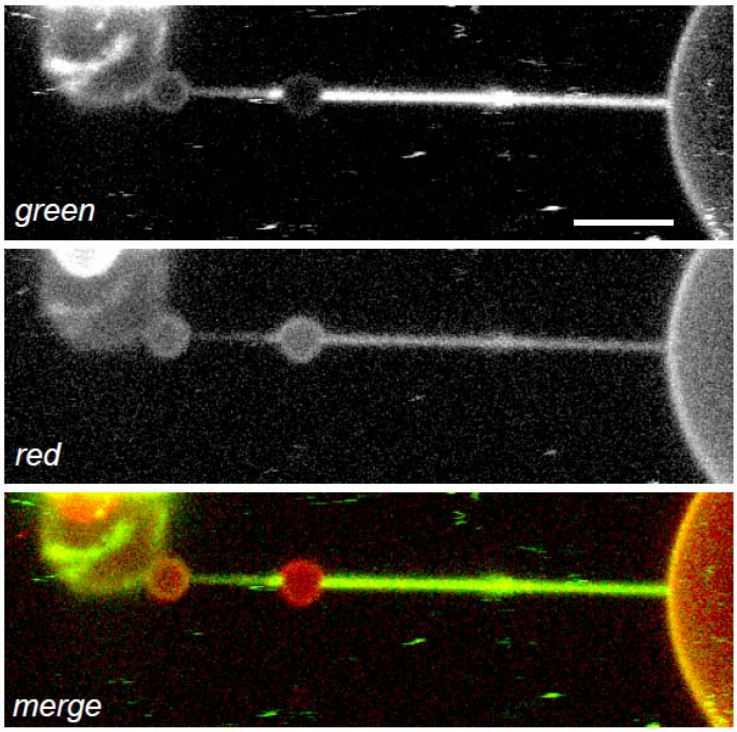


***Figure S4.*** Depletion of ENTH-GFP from low curvature swellings developed on tethers corroborates tether intensity curvature partitioning measurements. In this example, with 5 mol% $PIP_2$-containing POPC vesicles, swelling occurred during a tension ramp, although equivalent spontaneous transformations have also been observed. Such severe cases of apparent mechanical instabilities were not included in quantitative intensity measurements of the main text. Tension was subsequently lowered, and during a tether length change enforced by displacing the aspirated bead away from the vesicle, a second swelling arose. The image shows an *xyz* reconstruction of the two swellings at $\sigma$ = 0.09 mN/m. Bar: 5 μm.

*Supporting References*


1. *Tian, A.; Johnson, C.; Wang, W.; Baumgart, T., Line Tension at Fluid Membrane Domain Boundaries Measured by Micropipette Aspiration. Physical Review Letters* ***2007,*** *98, (20), 2081021 - 2081024.*
2. *Tian, A.; Baumgart, T., Sorting of lipids and proteins in membrane curvature gradients. Biophysical Journal* ***2009,*** *96, 2676 - 2688.*
3. *Kozlov, M. M.; Helfrich, W., Effects of a Cosurfactant on the Stretching and Bending Elasticities - a Surfactant Monolayer. Langmuir* ***1992,*** *8, (11), 2792-2797.*
4. *Sorre, B.; Callan-Jones, A.; Manneville, J. B.; Nassoy, P.; Joanny, J. F.; Prost, J.; Goud, B.; Bassereau, P., Curvature-driven lipid sorting needs proximity to a demixing point and is aided by proteins. Proceedings of the National Academy of Sciences of the United States of America* ***2009,*** *106, (14), 5622-5626.*
5. *Tian, A. W.; Capraro, B. R.; Esposito, C.; Baumgart, T., Bending Stiffness Depends on Curvature of Ternary Lipid Mixture Tubular Membranes. Biophysical Journal* ***2009,*** *97, (6), 1636-1646.*
6. *Leibler S., Curvature Instability in Membranes. Journal de Physique* ***1986,*** *47, (3), 507 - 516.*
7. *Kucerka, N.; Tristram-Nagle, S.; Nagle, J. F., Structure of fully hydrated fluid phase lipid bilayers with monounsaturated chains. Journal of Membrane Biology* ***2005,*** *208, (3), 193-202.*
8. *Hochmuth, R. M.; Wiles, H. C.; Evans, E. A.; Mccown, J. T., Extensional Flow of Erythrocyte-Membrane from Cell Body to Elastic Tether .2. Experiment. Biophysical Journal* ***1982,*** *39, (1), 83-89.*